Available online at www.sciencedirect.com
SCIENCE DIRECT®
Physica E 22 (2004) 761–766
PHYSICA E
www.elsevier.com/locate/physe

Confined electron crystals and Rydberg states on liquid helium

P. Glasson[a], E. Collin[a,b], P. Fozooni[a], P.G. Frayne[a], K. Harrabi[a], W. Bailey[a], G. Papageorgiou[a], Y. Mukharsky[b], M.J. Lea[a,*]

[a] *Department of Physics, University of London, Royal Holloway, Egham, Surrey TW20 0EX, UK*
[b] *CEA, Saclay, France*

Abstract

Experiments are in progress to measure and control the quantum states of surface state electrons on liquid helium, both individually and in arrays, for potential use as qubits. This requires the fabrication of novel electronic devices using microstructured substrates, the excitation of Rydberg states using millimetric microwaves and the detection of individual electrons and their quantum states. This paper presents some preliminary experimental results.

PACS: 73.20.−r; 73.50.Fq

Keywords: Electrons on helium; Qubits; Microwave absorption

1. Introduction

Electrons on the surface of liquid helium have been an interesting but rather esoteric field of research for many years. Platzman and Dykman [1] suggested that individual electrons localized on the surface of liquid helium could be used as qubits. The $|0>$ and $|1>$ states would be the ground and first excited Rydberg states in the vertical attractive potential well from the image charge in the helium. In this paper, we describe three precursor experiments to electronic qubits on helium: the fabrication of electronic devices on helium, the microwave excitation of Rydberg states and the detection of trapped electrons using a single-electron transistor.

2. Electronic devices on helium

2.1. Fabrication

Electronic devices have been fabricated to study electrons in confined geometries [2,3] as shown in Fig. 1. Electrodes were patterned in gold on a GaAs substrate using UV and e-beam lithography. Microchannels, 16 μm wide and 1.8 μm deep, were defined in a PMMA resist, whose upper surface was covered with a gold guard electrode.

The microchannels are filled with liquid helium, held by surface tension. Free electrons from a pulsed filament are held on the helium by DC bias potentials on the electrodes.

These structures and devices are similar to the technical requirements for electronic qubits, which need to be in potential wells about 1 μm apart. This determines the required helium depth and the scale of sub-surface electrodes for biasing and control.

* Corresponding author. Tel.: +44-1784-443485; fax: +44-1784-472794.
E-mail address: m.lea@rhul.ac.uk (M.J. Lea).

1386-9477/$ - see front matter
doi:10.1016/j.physe.2003.12.116

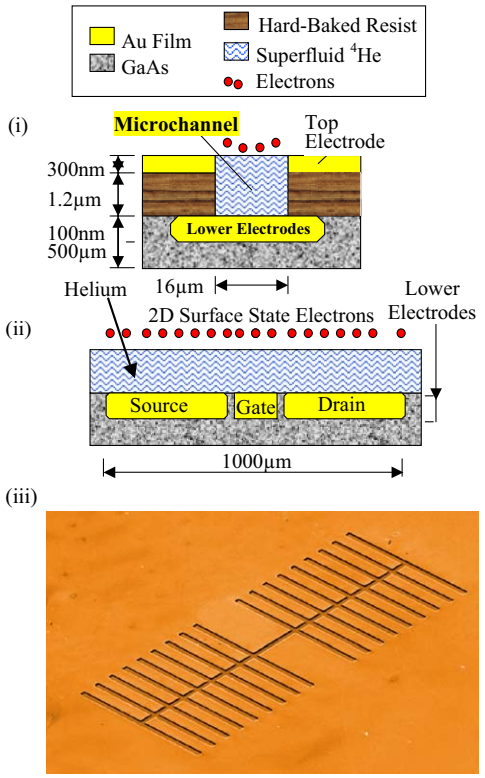

Fig. 1. Electronic FET, showing helium microchannels, electrons and electrodes. (i) channel cross-section, (ii) electrodes cross-section, (iii) photograph. The comb structure under the source and drain electrodes increases the capacitative coupling to the electrons.

2.2. Electronic FET

The device shown in Fig. 1 acts as an AC coupled field effect transistor (FET). An audio-frequency (1–20 kHz) voltage $V_0 \exp(i\omega t)$ applied to the source electrode capacitatively couples to the electrons. The AC current flowing to the drain is measured by a lock-in amplifier. The gate electrode, below the central channel, depletes or enhances the carrier density above it and switches off the source–drain current I_{sd} (Fig. 2). The intrinsic width of the cut-off region is small; the width is the peak-to-peak electron potential swing $\sqrt{2V_0}$. The total number of electrons above the gate (10×60 μm) is typically about 600 in the conducting state and far fewer near cut-off.

Above 1 K, the resistance of the device decreases exponentially as the temperature falls, as the mobility

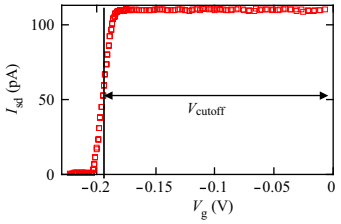

Fig. 2. The AC source–drain current $|I_{sd}|$ versus the DC gate voltage V_g, showing the cut-off due to the depletion of electrons over the gate.

is limited by scattering from ^{4}He vapor atoms. This shows that electron scattering from trapped charge or random potentials is small. The electrons are a good 2D classical Drude conductor.

2.3. Non-linear effects below 1 K

Below 1 K, the situation changes dramatically. The resistance of the device *increases* again as the temperature falls and a series of non-linear transport phenomena occur. The origin of these effects is thought to be electron–electron interactions in this strongly interacting system, which produce spatial order in the electrons. Electrons on bulk helium form a classical 2D Wigner crystal, which is modified in a confined geometry. In particular, molecular dynamic simulations [4] show that electrons in a microchannel can form discrete lines parallel to the edges, above the normal melting temperature. At lower temperatures, edge reconstruction of the crystal may occur [5]. A key feature of electrons on helium is that this order can be reflected directly in the transport properties. Moving the crystal generates ripplons on the helium surface. Coherent Bragg enhancement of the ripplon scattering occurs when the crystal moves at v_1, the ripplon phase velocity at the reciprocal lattice wave vector [6]. The resultant drag force increases, until the *ripplon barrier* is exceeded and the electrons decouple from the surface with $v \gg v_1$. This gives an "N-shaped" V–I characteristic for the electrons, with negative differential resistance. The moving crystal is dynamically pinned at velocity v_1.

Fig. 3 shows the non-linear voltage drop V along a microchannel at 0.52 K as a function of the current I_{sd} (proportional to the electron velocity amplitude v). Above a linear region at low currents, the voltage

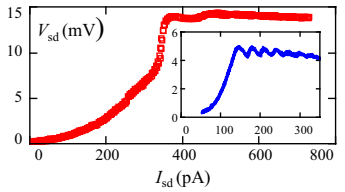

Fig. 3. The V–I characteristic at 0.52 K. For AC excitation, the voltage drop along the channels $V = V_0 \sin\phi$, where ϕ is the phase shift of the current I_{sd} away from purely capacitative coupling. Inset: resistance oscillations close to the nominal melting temperature.

rises rapidly to a critical value where it becomes constant. The constant V region is a characteristic of NDC which becomes unstable to the formation of current filaments [7]. A simple model in which high electron velocity edge currents grow at the expense of a slower central region, strongly coupled to the surface, gives a reasonable account of the experiments. A key parameter is the ripplon phase velocity v_1 (about 7 m/s for the densities used).

The inset shows periodic oscillations in the resistance, as discussed in Ref. [3]. The oscillations are most pronounced near the nominal melting temperature. We associate these with the progressive decoupling of ordered lines of electrons as the electron current increases.

At lower temperatures, other effects are observed, including a rapid fall in the low velocity mobility, random jumps and instabilities. Some of these are similar to effects seen with NDC in semiconductors [7] and presumably come from states of dynamical order in the electron system.

The relevance of these results for the development of qubits is that we have demonstrated the fabrication of devices using electrons on suspended films of helium. Small numbers of electrons can be stored and manipulated. Below 1 K, electron–electron interactions produce spatially ordered electrons, which can be statically or dynamically pinned.

3. Rydberg states of electrons on helium

3.1. Microwave absorption

The vertical potential well for a surface state electron is $V(z) = -K/z + eE_z z$, where the first term is the

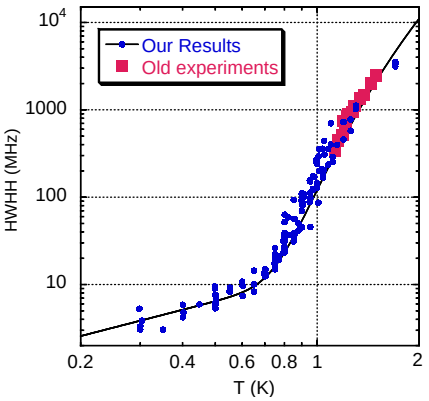

Fig. 4. The temperature-dependent contribution to the line width $\gamma(T)$ at 189.6 GHz. A linear temperature dependence was assumed below 0.8 K, as in the theory (full line) [10].

Coulomb interaction from the image charge in the helium and E_z is the applied electric field. This gives a series of Rydberg energy levels (quantum number m). These are hydrogenic for $E_z = 0$, with $E_m = -R_e/m^2$ (Rydberg energy $R_e = 0.67$ meV) but can be Stark shifted, and tuned, by E_z. We have extended measurements [8] of the temperature-dependent contribution to the resonant absorption line width $\gamma(T)$ from the ground state to the first excited state, at $f_{12} = \omega_{12}/2\pi$, to below 1 K [9]. We observed absorption saturation, power broadening and Coulomb effects. Measurements were made for electrons on bulk helium using a Gunn diode microwave source (165–195 GHz) and a Putley bolometric detector, by varying E_z to sweep through the resonance at a fixed microwave frequency.

The dominant contribution to the experimental line width below 0.5 K comes from inhomogeneous broadening due to spatial variations in E_z. However, the line shape broadens as the temperature increases and the temperature-dependent contribution $\gamma(T)$ can be accurately deduced by fitting the data to the convolution of a Gaussian, width $\gamma(T)$, and the low-temperature limit of the inhomogeneous line width. The results for $\gamma(T)$ are shown in Fig. 4, compared with previous measurements [8] and the theory by Ando [10] which gives $\gamma(T) = AT + BN_{gas}$ where N_{gas} is the number density of ^{4}He vapor atoms.

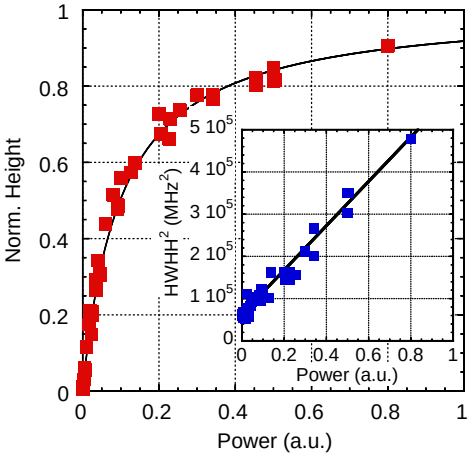

Fig. 5. Absorption saturation $\alpha(P)$ at 1 K for 189.6 GHz. Inset: power broadening data γ_P^2 (half-height-full-width) versus P where the inhomogeneous broadening has been subtracted.

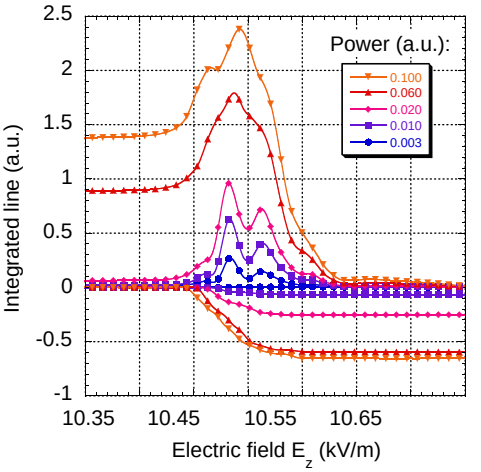

Fig. 6. The integrated line shape of the microwave absorption at 500 mK, showing the real (>0) and imaginary (<0) components of the offset at 0.5 K for various power levels. The integration zero has been chosen on the right (on the left) for the real (imaginary) signals for display purposes. The relative power was measured by chopping the c.w. microwaves and reading the Putley detector output with a lock-in amplifier.

3.2. Absorption saturation and power broadening

If the microwave power is increased, then absorption saturation and power broadening are observed. Because of the non-harmonicity of the Rydberg levels, the resonant absorption corresponds to a two-level system (a vital feature for qubits) and the power absorption α becomes [11]

$$\alpha = \frac{0.5N\gamma\Omega^2}{\delta^2 + \gamma^2 + \gamma\tau\Omega^2}, \qquad (1)$$

where N is the number of electrons, $\delta = \omega - \omega_{12}$, τ is the excited state lifetime, $\Omega = eE_{\mathrm{RF}}z_{12}/\hbar$ is the Rabi frequency, E_{RF} is the microwave field amplitude and z_{12} is the dipole length of the transition. Absorption saturation and the power broadening of the line width are shown at 0.9 K in Fig. 5. We can deduce two significant results for qubits. First, saturation shows that we are exciting a large fraction ρ of electrons into the excited state. The maximum excitation for the data in Fig. 5 is $\rho = 0.49$, just below the theoretical maximum of 0.5 for thermal equilibrium. Since $\Omega^2 \propto P$, the microwave power, we can also deduce the maximum Rabi frequency for Fig. 5 as about 260 MHz, well within the required range [1].

3.3. Coulomb effects

Below 0.5 K, some hysteresis was observed in the microwave absorption lines. The field E_z, and hence f_{12}, was modulated at a low frequency ($f_{\mathrm{mod}} = 1$ kHz) and the differential absorption measured with a lock-in amplifier. The absorption line was found by numerical integration. At low temperatures and higher powers, the integrated line showed an offset and an imaginary component, with respect to f_{mod}, as shown in Fig. 6. This unusual result means that each sine-wave modulation cycle sees different absorption for increasing and decreasing E_z, i.e. hysteresis.

The hysteresis is power dependent. Because of the Coulomb interaction between electrons, an excited electron will increase the resonant frequency of its neighbors (this would give the interactions for qubits). For our typical electron density of 0.2×10^{12} m^{-2}, the Coulomb shift Δf_{C} is about 12 MHz for the excitation of one nearest neighbour. A mean-field calculation would give $\Delta f_{\mathrm{C}} \propto \rho$, introducing a non-linear term into Eq. (1). When $\gamma(T)$ becomes less than the Coulomb shift, the Lorenztian response will become hysteretic for modulation amplitudes of f_{12} greater than Δf_{C}, which was normally the case. The offset of the integrated line shape is consistent with our estimates of Δf_{C}.

3.4. Microwaves and qubits

The measured temperature-dependent contribution to the line widths is small. However, Dykman and Platzman [1] show that the localization of electrons should reduce the line widths even further. Electrons as qubits would be addressed by microwave pulses. The important parameters for qubits are the Rabi frequency (determining the clock rate), the excited state lifetime T_1 (in NMR terms) and the decoherence time T_2. Both T_1 and T_2 will be proportional to the inverse microwave line width $1/\gamma$, though the proportionality will depend on the mechanism.

A consistent analysis has been developed to include power saturation, non-linear effects, finite-modulation hysteresis and inhomogeneous broadening. This enables us to determine the excited state lifetime τ and the line width γ independently, from the high power data. The values for the temperature-dependent contribution $\gamma(T)$ agree well with the low power measurements, as shown in Fig. 4. But we also find a lifetime τ, which is *independent* of $\gamma(T)$ at low temperatures. For a particular scattering mechanism, $\gamma\tau = 2\gamma/\gamma_{\mathrm{inel}}$ where γ_{inel} is the inelastic, or lifetime contribution to the total line width γ and hence $\tau \propto 1/\gamma$. For gas–atom scattering we estimate $\gamma\tau = 2.9$ at the holding field E_z used, though the ratio has not been calculated explicitly for ripplon scattering. Hence a constant τ also implies a constant line width, which is comparable with the measured inhomogeneous broadening (and cannot be distinguished from it). The origin of this effect is unknown but it could be related to the electron–electron or Coulomb interactions, analogous to the dipolar interactions in NMR. If the short lifetime has another origin and is also present for localised electrons, there will be adverse implications for qubit operation.

4. Detecting electrons with an SET

Several techniques have been suggested for detecting surface state electrons as qubits, and to read out their quantum states [1]. We have chosen to use a single-electron transistor (SET), at least in the development phase, to enable the characteristics of electron traps and qubit properties to be determined. An SEM photograph of a prototype device is shown in Fig. 7.

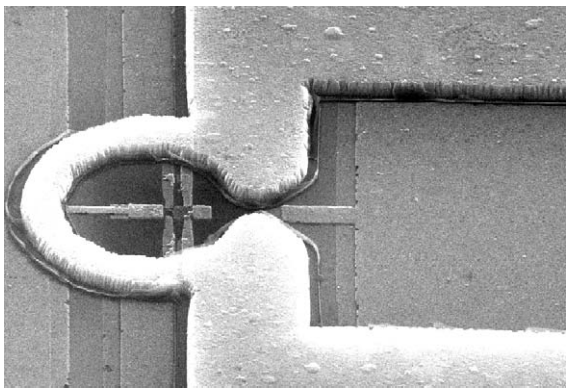

Fig. 7. An SET for detecting trapped electrons on a pool of helium. The electrodes on the right form an electron reservoir with an injector electrode.

The device was made on a Si substrate with a SiO_2 buffer layer using e-beam lithography and shadow evaporation to fabricate an SET inside an aluminium ring. The ring defines a pool of helium, 0.5 μm deep and 2.5 μm diameter for an electron trap. Coulomb blockade oscillations in the SET source-drain current are generated by sweeping gate and guard electrodes. Electrons are stored in a microchannel reservoir and, in principle, fed into the electron trap through an injector. Trapped electrons induce a shift in the CBO phase. Preliminary results indicate that electrons can be trapped and detected. Experiments are in progress to confirm these conclusions and to control the trapping process.

In principle, such an SET can also detect the quantum state of a surface state electron. The first excited Rydberg state lies further above the helium surface and the induced charge in the SET island should change by about $0.04e$ [1].

5. Conclusions

We have demonstrated that surface state electrons on helium can be trapped and manipulated in microfabricated electronic devices. The excitation of Rydberg states by resonant microwave absorption is feasible and high excitation levels can be achieved. The line width is small and should be further reduced for localized electrons. A single-electron transistor (SET) has been developed for the detection of surface-state

electrons on helium, though only preliminary results are available so far.

For the future, high-frequency, or RF-SETs, have been shown to have sufficient sensitivity and speed to resolve real-time qubit events for trapped electrons and twin SETs allow discrimination against charge noise [12]. A number of experimental groups are now investigating the SET read-out of qubit states, including electrons on helium. As well as charge-based qubits, it has also been suggested that the spin of surface state electrons would be an excellent alternative qubit state [13]. ESR techniques would be used for qubit control. Interactions would take place through dipole–dipole interactions and would be rather slow (10 ms timescale). There is little doubt that the quantum states of surface-state electrons on helium will be actively studied in the future. The concept of using free electrons for quantum information processing is most enticing.

Acknowledgements

E. Collin and K. Harrabi acknowledge the financial support provided through the European Community's Human Potential Programme under contract HPRN-CT-2000-00157, *Surface Electrons*. We thank the EPSRC and the EU Network on *Surface Electrons* for financial support, and John Taylor, Alan Betts, Francis Greenough and others for technical assistance.

References

[1] P.M. Platzman, M.I. Dykman, Science 284 (1999) 1967;
M.I. Dykman, P.M. Platzman, Fortschr.Phys. 48 (2000) 1095;
M.J. Lea, P.G. Frayne, Yu. Mukharsky, Fortschr. Phys. 48 (2000) 1109;
M.I. Dykman, P.M. Platzman, P. Seddighrad, 2002, cond-mat/0209511.
AJ. Dahm, et al., J. Low Temp. Phys. 126 (2002) 709.
[2] Y.Z. Kovdrya, Low Temp. Phys. 29 (2003) 77, Private communication, 2003.
[3] P. Glasson, et al., Phys.Rev.Lett. 87 (2001) 176802.
[4] K.M.S. Bajaj, R. Mehrotra, Physica B 194–196 (1994) 1235.
[5] H.A. Fertig, R. Cöté, A.H. MacDonald, S. Das Sarma, Phys. Rev. Lett. 69 (1992) 816.
[6] M.I. Dukman, Y.G. Rubo, Phys. Rev. Lett. 78 (1997) 4813;
W.F. Vinen, J. Phys.: Condens. Matter 48 (1999) 9709.
[7] H. Thomas (Ed.), Non-Linear Dynamics in Solids, Springer, Berlin, 1992.
[8] C.C. Grimes, T.R. Brown, M.L. Brown, C.L. Zipfel, Phys. Rev. B 13 (1976) 140;
A.P. Volodin, V.S. Edel'man, Sov. Phys. JETP 54 (1981) 198;
D.K. Lambert, P.L. Richards, Phys. Rev. B 23 (1981) 3382.
[9] E. Collin, et al., Phys. Rev. Lett. 89 (2002) 245301.
[10] T. Ando, J. Phys. Soc. Japan 44 (1978) 765.
[11] R. Loudon, The Quantum Theory of Light, 3rd Edition, Oxford Science, Oxford, 2000.
[12] K. Bladh, et al., Phys. Scr. T 102 (2002) 167;
T.M. Buehler et al., 2002, cond-mat/0302085
T.M. Buehler, et al., Appl. Phys. Lett. 82 (2003) 577.
[13] S.Lyon, Private communication, 2003.